



Experiment Report Form

The double page inside this form is to be filled in by all users or groups of users who have had access to beam time for measurements at the ESRF.

Once completed, the report should be submitted electronically to the User Office using the **Electronic Report Submission Application**:

<http://193.49.43.2:8080/smis/servlet/UserUtils?start>

Reports supporting requests for additional beam time

Reports can now be submitted independently of new proposals – it is necessary simply to indicate the number of the report(s) supporting a new proposal on the proposal form.

The Review Committees reserve the right to reject new proposals from groups who have not reported on the use of beam time allocated previously.

Reports on experiments relating to long term projects

Proposers awarded beam time for a long term project are required to submit an interim report at the end of each year, irrespective of the number of shifts of beam time they have used.

Published papers

All users must give proper credit to ESRF staff members and proper mention to ESRF facilities which were essential for the results described in any ensuing publication. Further, they are obliged to send to the Joint ESRF/ ILL library the complete reference and the abstract of all papers appearing in print, and resulting from the use of the ESRF.

Should you wish to make more general comments on the experiment, please note them on the User Evaluation Form, and send both the Report and the Evaluation Form to the User Office.

Deadlines for submission of Experimental Reports

- 1st March for experiments carried out up until June of the previous year;
- 1st September for experiments carried out up until January of the same year.

Instructions for preparing your Report

- fill in a separate form for each project or series of measurements.
- type your report, in English.
- include the reference number of the proposal to which the report refers.
- make sure that the text, tables and figures fit into the space available.
- if your work is published or is in press, you may prefer to paste in the abstract, and add full reference details. If the abstract is in a language other than English, please include an English translation.



Experiment title: Self-assembly of low molecular weight and polymeric materials for organic electronic devices

Experiment number:
SC2647

Beamline: ID02	Date of experiment: from: 13.7.10 to: 16.7.10	Date of report: 14.9.2010
Shifts: 9	Local contact(s): Michael Stzucki	<i>Received at ESRF:</i>

Names and affiliations of applicants (* indicates experimentalists):

Dr. Sven Huettnner*, Cavendish Laboratory, University of Cambridge

Dr. Michael Sommer, Melville Laboratory, University of Cambridge

Prof. Ullrich Steiner, Cavendish Laboratory, University of Cambridge

Prof. Mukundan Thelakkat, Applied Functional Polymers, Universität Bayreuth

Further experimentalists:

Dr. Peter Kohn*, Experimentelle Polymerphysik – Prof. Thomas Thurn-Albrecht, Universität Halle

Andreas Lang*, Applied Functional Polymers, Universität Bayreuth

Ruth Lohwasser*, Applied Functional Polymers, Universität Bayreuth

Jens Balko*, Experimentelle Polymerphysik – Prof. Thomas Thurn-Albrecht, Universität Halle

Report:

Following the proposal of SC2647 we have investigated several n-type low molecular weight and polymeric systems and especially p-type poly(3-hexylthiophene), materials that are suitable for the application in organic electronic devices such as organic field-effect transistors (OFET) or organic photovoltaics (OPV).

A crucial parameter in semiconducting polymers is their crystallinity. It decides on the planarity of the conjugated backbones, crystal sizes and grain boundaries. These parameters, in return, influence electro-optical properties such as the charge carrier mobility or the absorption and emission spectra. Therefore, the structural information gained from these measurements allows us to draw strong correlations to their electrical and optical properties. The combination of SAXS and WAXS measurements provides a broad q-range to obtain the structural information that is prevalent in different hierarchical levels of semicrystalline polymers. Fig. 1 summarizes the different hierarchical structures we could obtain in poly(perylene bisimide acrylate) (PPerAcr), a n-type side-chain crystalline polymer developed in the group of Prof. M. Thelakkat. The π - π stacking takes place in the range of 3.5 Å, and the strong π - π interactions lead to the formation of stacks that arrange within a two-dimensional lattice ranging around ~2nm. If this polymer is incorporated into a block copolymer, the microphase separation of the block copolymer induces a further hierarchy on the order of ~15nm. Fig. 2 shows the structures of poly(3-hexylthiophene) (P3HT). The conjugated polymer exhibits π - π -stacking in one direction, and forms lamellae that are separated by alkyl chains. On a larger length scale, crystalline and amorphous domains form a further periodicity on the order of ~10nm, called long period (L).

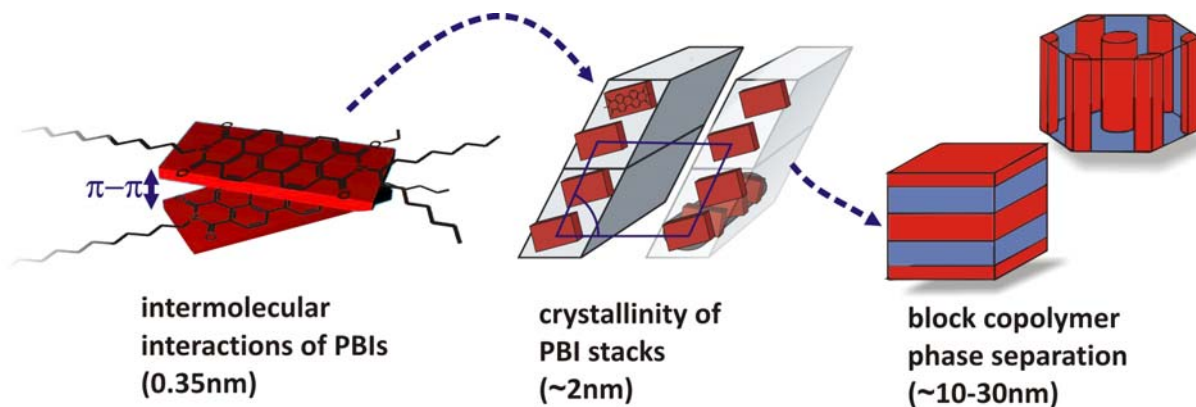


Fig 1- Structure formation on different hierarchical length scales in PPerAcr and related block copolymers. Intermolecular π - π -stacking ranges around 3.5Å.

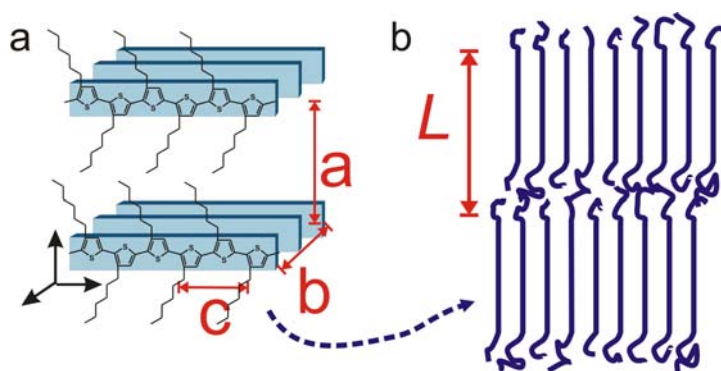


Fig 2- Crystallinity of P3HT leading to structure formation on different length scales

In this report we will give a short overview of measurements carried out on perylene bisimides and poly(3-hexylthiophenes):

- 1) polymers carrying perylene bisimides prepared by “click” chemistry
- 2) poly (perylene bisimide acrylate)
- 3) perylene diester benzimidazole
- 4) poly(3-hexylthiophene)s with different end groups
- 5) crystallisation of poly(3hexylthiophene)s correlated with absorption spectroscopy
- 6) behaviour of poly(3-hexylthiophene)s during controlled solvent vapour exposure
- 7) first results on crystallisation of defect-free poly(3-hexylthiophene)s

1) Polymers carrying perylene bisimide prepared by “click” chemistry

Semiconductor polymers carrying perylene bisimides (PBI) have been used as n-type materials in amorphous-crystalline^{1,2,3} as well as in double crystalline⁴ block copolymers for photovoltaic cells. These polymers often exhibit broad molecular weight distributions. By the use of so-called “click” chemistry⁵ we are able to synthesize side-chain polymers carrying perylene bisimide with excellent molecular weight distributions as low as 1.08 and molecular weights up to 60 000 g/mol. Also, the polarity of the pendant perylene bisimide can be varied as well as the length of the alkyl spacer between the PBI unit and the polymer backbone. Here we aim to determine the hierarchical structures of differently substituted perylene bisimide “click” polymers shown in Figure 3a). Figure 3b) shows the diffraction patterns of these materials at RT. Polymers **PBI 15** and **PBI 16** show three distinct reflections with a ratio of 1:2:3, indicating a lamellar

¹ S. M. Lindner, M. Thelakkat, *Macromolecules* 2004, **37**, 8832.

² S. M. Lindner, S. Hüttner, A. Chiche, M. Thelakkat, G. Krausch, *Angew. Chem. Int. Ed.* 2006, **45**, 3364.

³ M. Sommer, S. M. Lindner, M. Thelakkat, *Adv. Funct. Mater.* 2007, **17**, 1493.

⁴ M. Sommer, A. Lang, M. Thelakkat, *Angew. Chem. Int. Ed.* 2008, **47**, 7901.

⁵ A. S. Lang, A. Neubig, M. Sommer, M. Thelakkat, *Macromolecules* 10.1021/ma100708h.

2D order. Polymer **PBI 17** with the longest alkyl spacer does not show crystalline order. All polar polymers **PBI 18-20** do not show any crystalline order either. This indicates that PBI polymers with polar swallow-tails do not show crystallinity in any way, and that the crystallinity of PBI polymers with apolar swallow-tails is strongly dependent on the spacer length (Figure 3c).

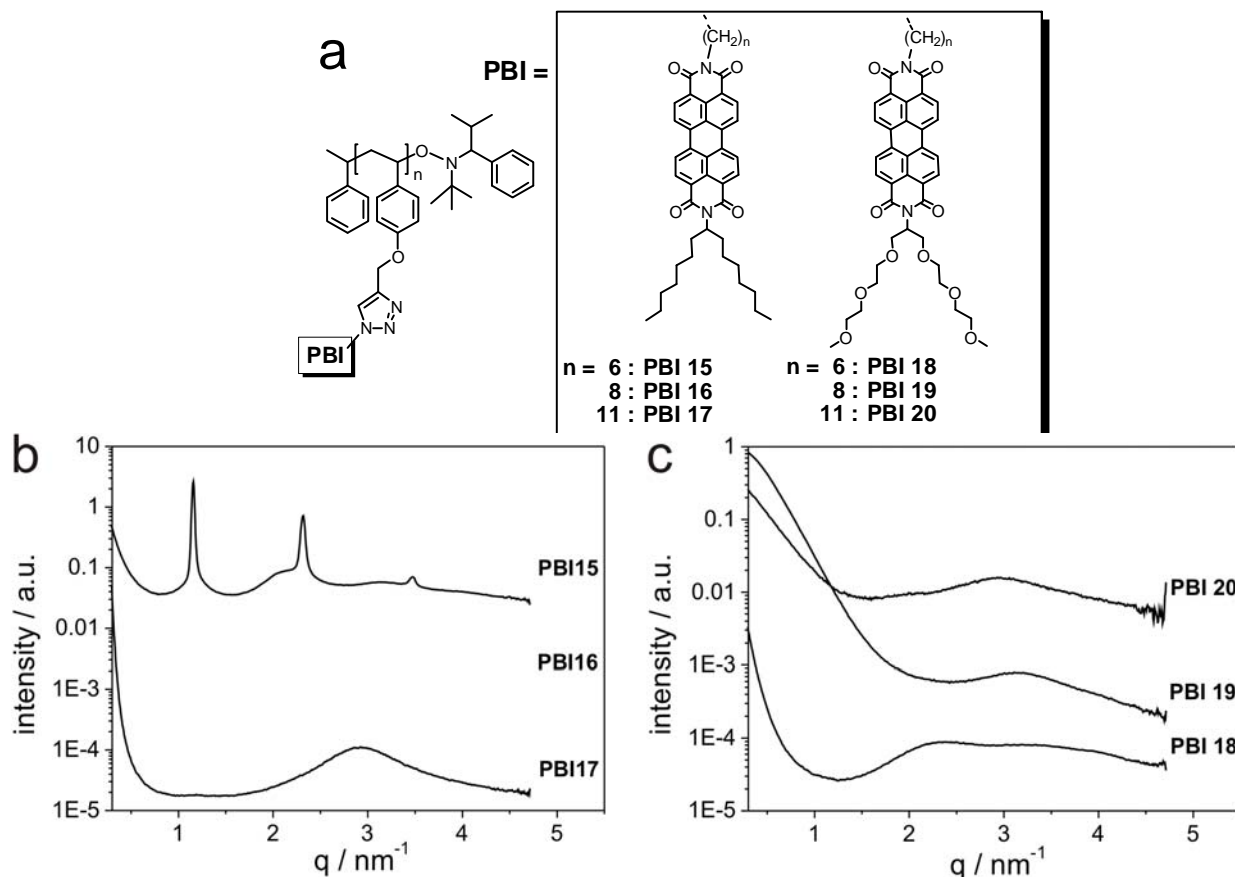


Fig 3- a) Chemical structure of PBI “click” polymers PBI 15-17 (apolar) and PBI 18-20 (polar). b) SAXS diffraction pattern of PBI 15-17 showing a structure dependence on spacer length. c) SAXS diffraction pattern of PBI 18-20 showing only amorphous halos in all three polymers.

2) Temperature dependent measurements of PPerAcr

The opportunity to obtain temperature dependent data helps us to understand and correlate structural results with those obtained from opto-electronical measurements. The crystallinity and the aggregation of the perylene bisimide units is strongly influenced by the sample processing. In order to investigate the effect of a different sample preparation we performed X-ray scattering experiments at different temperatures and after different annealing procedures. Crystalline PPerAcr - as it appears after cooling it slowly (~ 10 K/min from the melt (Figure 4b-VIa) - shows features of the π - π stacking of the perylene bisimide moieties of 3.5Å at $q = 17.8 \text{ nm}^{-1}$. The crystalline perylene bisimides form a monoclinic lattice with lattice parameters of $a = 3.5 \text{ nm}$ and $b = 2.2 \text{ nm}$ having an angle of $\gamma = 60.5^\circ$. The first order peaks are indicated in Figure 4b-VIa followed by convolution of higher order peaks in the range from $q = 5-8 \text{ nm}^{-1}$, and a broad amorphous halo originating from the alkyl chains ($q = 9-16 \text{ nm}^{-1}$). The extend of crystallinity depends on the kinetics and the temperature of the annealing procedure which is investigated in the following: Figure 4a shows a temperature program as it has been proceeded during in-situ X-ray measurements, of which exemplified data is shown in Figure 7b. The series starts with a bulk sample that has been annealed by solvent vapour before. The fast evaporation of the solvent molecules leads to a rather disrupted structure that can be seen in the broad peak between $q = 2-4 \text{ nm}^{-1}$, where no distinct peaks can be resolved. When the sample is heated to a temperature still

below the melting temperature, first rearrangements of amorphous parts take place already at a temperature of around

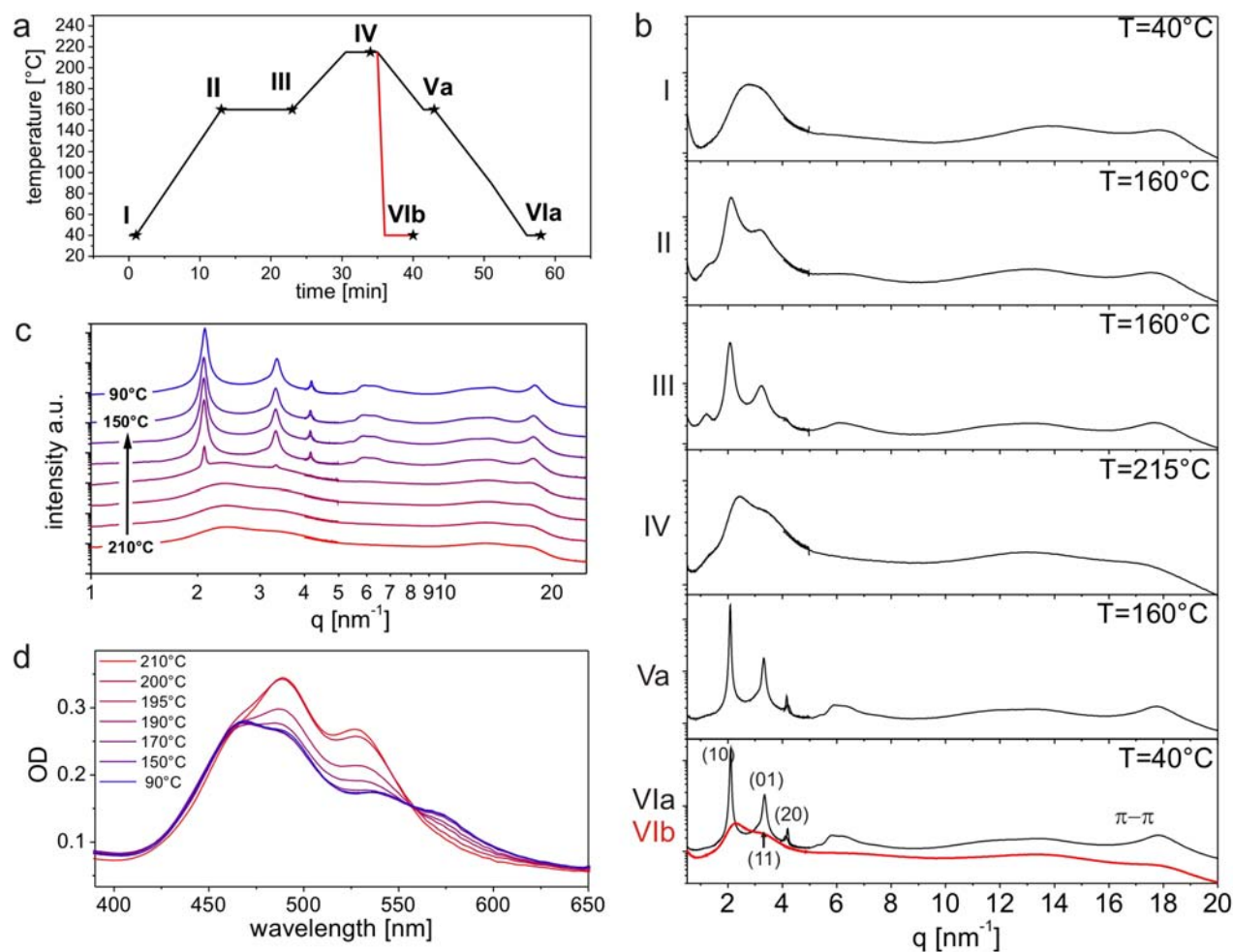


Fig 4 - Temperature dependent X-ray and absorption spectroscopy measurements of PPerAc. a) Temperature of the sample run. The stars indicate the points at which X-ray spectra are plotted in b). b) Combined small and wide angle X-ray spectra from PPerAc at selected temperatures: (I) after solvent vapour exposure at 40 °C; (II) at 160 °C; (III) after holding at 160 °C for 10 min; (IV) at 215 °C, where PPerAc is molten; (Va) at 160 °C after cooling from the melt at 10 K/min; (VIa) at 90 °C, which is identical to the measurement at 40 °C after cooling it further down from 160 °C at a rate of 10 K/min (black line); (VIb) at 40 °C after fast cool down (red curve). c) Selected X-ray measurements during cooling from the melt and d) corresponding absorption spectra taken from thin films at the same temperatures. The recrystallization is visible by the appearance of sharp features in the X-ray spectra and also by the enhanced formation of charge-transfer states.

130 °C. In the temperature scan, we kept the temperature at 160 °C for ten minutes. Figure 4b-II and III show the development shortly before and after the isothermic step. Interestingly, an enhancement of crystalline order is achieved already below the melting temperature. Also, an additional feature at $q=1.2 \text{ nm}^{-1}$ appears that is not directly related to the monoclinic lattice, and which we therefore attribute to a non-equilibrium appearance (structure sizes of 5.2 nm in real space). Local intermolecular rearrangements among the perylene bisimide moieties into larger and ordered crystalline structures occur below the melting temperature. PPerAc melts at $\sim 193 \text{ }^\circ\text{C}$ and the crystalline features disappear as figure 4b-IV shows: The peak for the intermolecular stacking disappears and a broad halo replaces the distinct crystalline features. The kinetics of recrystallisation determines the degree of crystallinity that is achieved depending on the cooling rate.

A qualitative comparison of the peak widths informs on the extend of the long range order in the bulk. Figure 4b-Va and VIa show the recrystallised PPerAc at a rate of 10 K/min, where we observed the highest crystallinity. Figure 4c shows intermediate steps of the cooling process and correlates them with absorption

spectra (Figure 4d) as measured in a film of PPerAcr. Upon cooling, the vibronic transitions decrease in oscillator strength together with a systematic increase of the low energy charge transfer feature where we find an isosbestic point at 558 nm. This provides direct experimental proof of the previously suggested correlation between oscillator strength at 590 nm and crystallinity in the bulk. Fast quenching from the melt with rates > 10 K/s, where the sample is quickly cooled on a metal block results rather in freezing of the molten state as Figure 4b-VIb (dashed line) shows. We have to note that the cooling rate for the X-ray samples that were supported by aluminum holders were higher than those on the glass substrates as used for spectroscopy later due to the 290 times higher thermal conductivity of aluminum.

The degree of aggregation not only influences the optical absorption but also the charge transport. We also measured field effect transistors with these materials after applying the same several annealing methods. These measurements allow extracting a value for the charge carrier mobility. The value calculated from field effect transistor measurements usually overestimates the bulk carrier mobility, but it offers an excellent method to compare the different annealing methods and the effect of perylene bisimide aggregation on the transport characteristics. The mobility after spin coating from chloroform- as determined from the saturation regime in OFETs - is as low as 10^{-5} cm^2/Vs and a similar value is deduced from the solvent vapour annealed samples (6.5×10^{-6} cm^2/Vs). Additional thermal annealing leads to a crucial increase of the mobility. After a low temperature annealing at 160°C , the as spun sample and the previously solvent vapour annealed sample reach mobilities of 9.9×10^{-4} cm^2/Vs and 6.8×10^{-4} cm^2/Vs , respectively. The thermally annealed sample at 215°C with fast quenching reaches mobilities up to 10^{-5} cm^2/Vs , while those quenched slowly reach higher mobilities of approximately 1.2×10^{-3} cm^2/Vs . Thus the charge aggregation of the perylene bisimides is important for the charge transport and the more time given for aggregation, the higher the charge carrier mobility.

3) Perylene diester benzimidazole

We investigated the discotic liquid crystalline compound perylene diester benzimidazole (PBI, Fig. 5a) as well as the corresponding polymer with acrylic backbone carrying PBI as a side chain. The polymer is to be used as electron accepting block (n-type) in donor-acceptor block copolymers for photovoltaic applications with P3HT as the hole conducting block (p-type).⁶

In order to reveal the phase behavior of this compounds we performed SAXS and WAXS measurements in the range from room temperature up to the isotropic melt. The WAXS pattern of the low molecular weight model compound during heating is shown in Fig. 5b indicating the transition of the liquid crystalline state to isotropic melt.

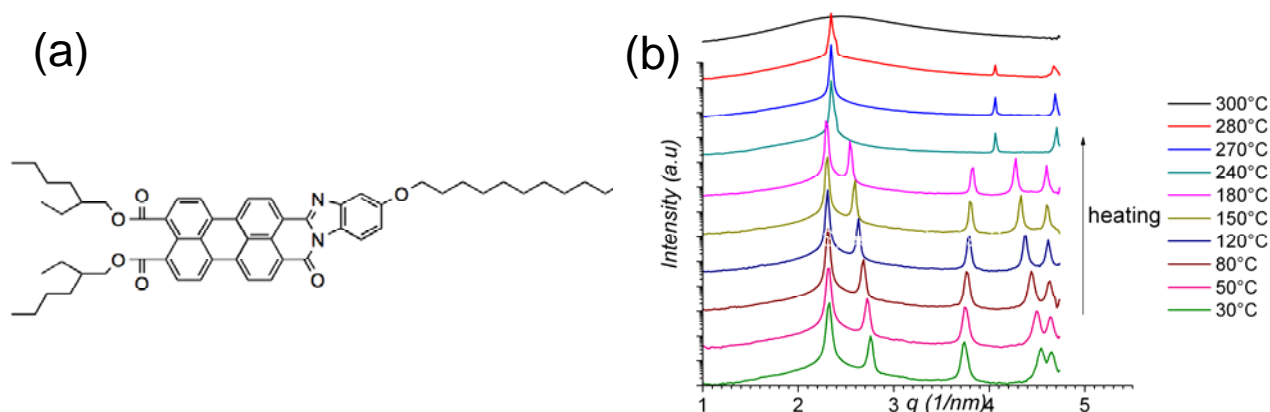


Fig 5 - a) Chemical structure of the model compound perylene diester benzimidazole and its b) temperature dependent WAXS pattern.

⁶ M. Sommer, S. Hüttner, U. Steiner and M. Thelakkat: *Influence of molecular weight on the solar cell performance of double-crystalline donor-acceptor block copolymers*, Appl. Physics Letters **95**, 183308 (2009)

A detailed evaluation of the structural evolution during heating and cooling is still under work. However up to now one can state that both components exhibit a columnar liquid crystalline phase due to the strong π - π interaction between stacking perylenes.

4) Chain length and end group dependent crystallisation of poly(3-hexylthiophenes)

Poly(3-hexylthiophene) (P3HT) is one of the most common hole conductors for organic electronic devices, like organic solar cells and organic field-effect transistors. Recently, we have shown that the introduction of carboxylic acid groups as chain ends allows the use of P3HT as a sensitizer in dye-sensitized solar cells.⁷ X-ray measurements showed that the multicarboxylation method used for functionalization resulted in a complete loss of crystallinity. The development of a new functionalization method for monocarboxylated P3HTs (P3HT-COOHs) lead to polymers with COOH anchoring groups, which were still semi-crystalline. A series of four polymers with and without COOH end groups were investigated during an earlier measurement time at the beamline ID2 at Grenoble. The results were submitted to *Macromolecules* and are currently in press.⁸ In this publication two additional low molecular weight functionalized and non-functionalized P3HTs (P3HT1 and P3HT1-COOH) were shown (Figure 6).

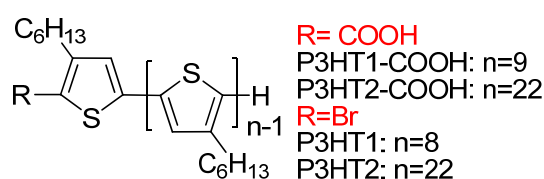


Fig 6 - Structures of the investigated polymers bearing different end groups.

These polymers possess melting temperatures untypical for main chain crystallization, which should have a transition at higher temperatures according to theoretical calculations. During this beam time, these polymers were analysed and the WAXS results are presented in Figure 7. The diffractograms indicate that the reduction of the molecular weight from 5000 g/mol (P3HT2 in Figure 6a) to 1500 g/mol (P3HT1 in Figure 7b) leads to a change in crystal structure as predicted by theory. The change of the end group from bromine for P3HT1 (Figure 7b) to a carboxylic acid group for P3HT1-COOH (Figure 7c) also modifies the crystal structure. While bromine end groups may have only sterical effects on the packing of P3HT, COOH groups have the ability to form hydrogen bonds and thus may behave different regarding molecular packing. The detailed structures still have to be evaluated.

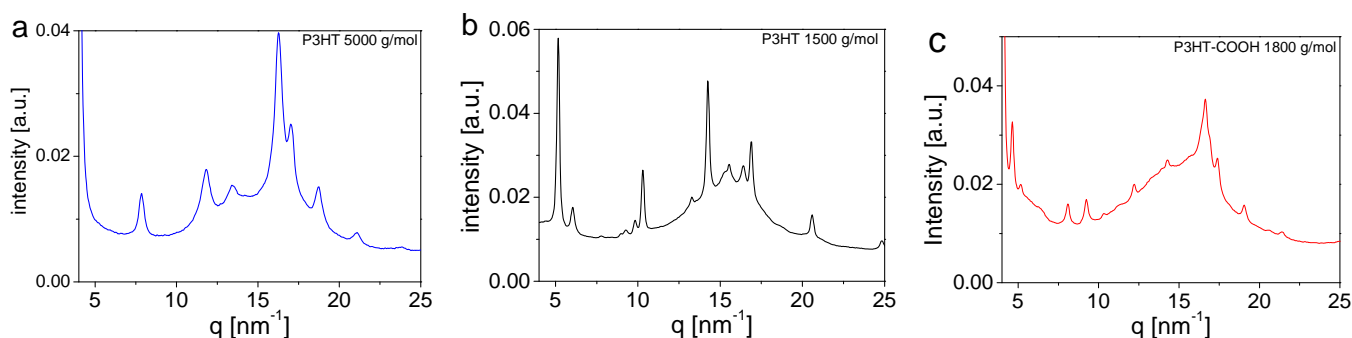


Fig 7 - WAXS diffractograms of a) P3HT2 with a number average molecular weight M_n of 5000 g/mol which shows typical reflexes for main chain crystallization b) P3HT1 with $M_n = 1500$ g/mol and c) P3HT1-COOH.

P3HT can transport charges via two different ways: intramolecular by conjugation along the chain and intermolecular by π - π -stacking. The carboxylic acid groups in these polymers allow for anchoring and thus orientation of polymer chains on the surface. The investigation of orientation dependent charge carrier mobilities might help to determine which transport mechanism mainly contributes to the charge transport. Thus, further GIWAXS measurements of anchored P3HT-COOHs are of interest. Analyses of the SAXS measurements indicate that the COOH groups also have an influence on the long period of the polymers. While carboxylated P3HT2-COOH and uncarboxylated P3HT2 with a molecular weight of 5000 g/mol show

⁷ Lohwasser, R.; Bandara, J.; Thelakkat, M. *J. Mater. Chem.* **2009**, *19*, 4126-4130.

⁸ Lohwasser, R.; Thelakkat, M. *Macromolecules* **2010**, in press.

the same crystal structure in WAXS, differences in the SAXS region are observed. After annealing of the samples above the melting temperature the uncarboxylated P3HT2 shows only one peak, while two broad features are observed for P3HT2-COOH (Figure 8). The origin of this is under investigation.

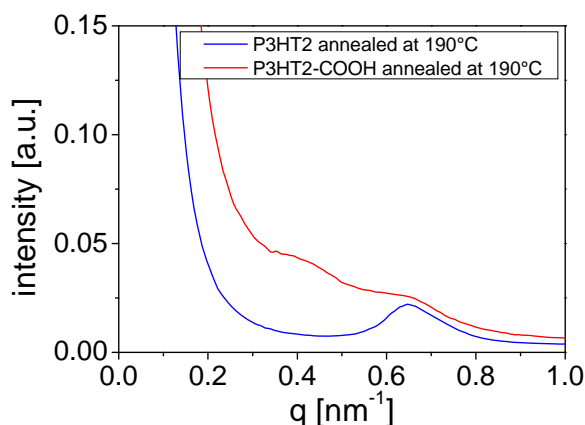


Fig 8 - Scattering curves of P3HT2 and P3HT2-COOH after annealing at 190°C.

5) Temperature and Molecular Weight Dependent Phase Behaviour of Poly(3-hexyl thiophene)

Poly(3-hexyl thiophene) is a common polymer semiconductor, often used as material or component in organic field effect transistors or solar cells. Despite of the extensive amount of work done on this material there are a number of important open questions concerning the structure and morphology. In Fig. 9 a schematic of the semicrystalline structure of P3HT is depicted.

Previous results^{9,10} indicated a layered, smectic phase of P3HT prior to the transition to isotropic melt during heating. A particular question of this study was whether this phase transition is a general effect also for higher molecular weights.

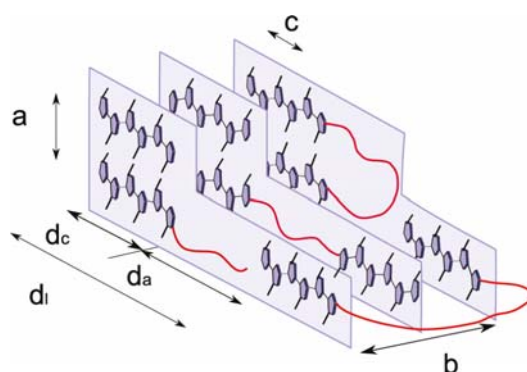


Fig 9 - In the schematic (not to scale, reprinted from [1]) the semicrystalline structure of P3HT is represented seen by the length d_c of the crystalline phase, the amorphous phase d_a and their sum the long period d_l . The lattice parameters a , b and c of the crystalline phase reflect the main chain to main chain distance, the ordering in π - π direction and along the main chain, respectively.

We performed temperature dependent scattering experiments on *bulk* samples of P3HT with four different molecular weights (5kDa, 20kDa, 27kDa, 34kDa) in order to elucidate the phase transitions taking place. We used chemically well defined samples, i.e. a very narrow distribution of molecular weights and a high degree of regiorregularity of the side chains.

² Hugger, S.; Thomann, R.; Heinzl, T.; Thurn-Albrecht, T. *Colloid Polym. Sci.* **2004**, 282, 932

¹⁰ Z. Wu, A. Petzold, T. Henze, T. Thurn-Albrecht, T. L. Lohwasser, M. Sommer, M. Thelakkat, *Macromolecules* **43**, 4646-4653 (2010)

The SAXS and WAXS measurements were needed to cover the whole range of structure occurring in P3HT. An overview of a series of diffraction patterns recorded during heating of the low molecular weight P3HT is given in Fig. 10a and 10b. A closer look at specific q-ranges (Fig.10c-e) reveals the transition from the crystalline phase still present at 160°C to the liquid-crystalline phase with smectic symmetry at 190°C. At this temperature only the (100) reflection at $q \sim 3.5 \text{ nm}^{-1}$ is left whereas the higher orders (Fig. 10d), the (020/002) reflection (Fig. 10e) as well as the bump at the lowest q (Fig. 10c) reflecting the semicrystalline morphology have vanished.

The measurements showed that the samples with higher molecular weights also exhibit a liquid-crystalline phase prior to melting, however the temperature range for the mesophase is much smaller. This result is represented in Fig. 4a. The phase transition is reversible as it is observed during cooling, too.

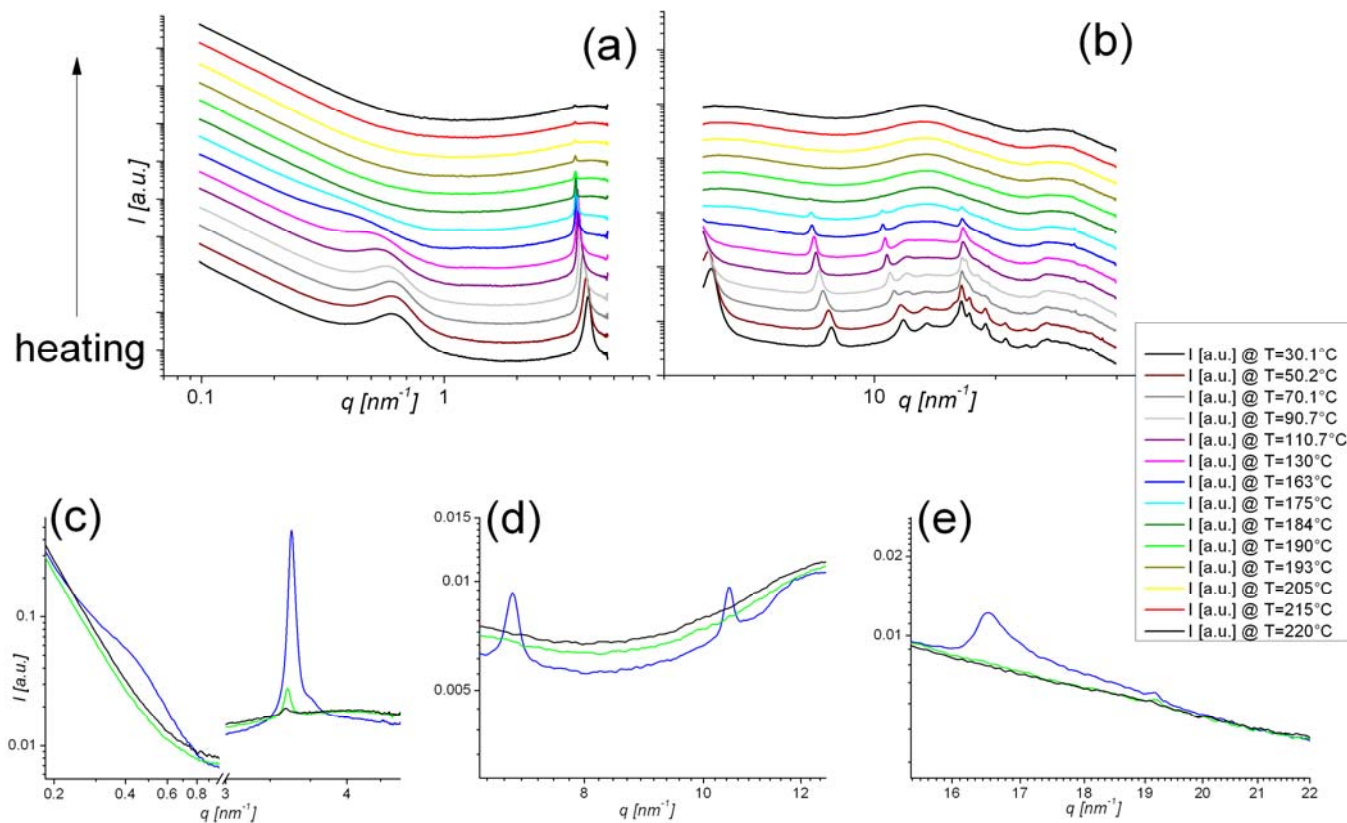


Fig 10 - (a) Small angle and (b) wide angle scattering patterns (shifted for clarity) for temperature dependent powder diffraction of the P3HT with a molecular weight of $M_n=5 \text{ kDa}$. (c) Reflection indicating the lamellar semicrystalline structure and (100) reflection with its (d) higher orders. (e) (020/002) reflection.

For higher molecular weights (20 kDa and higher) it is shifted to higher temperatures. For a molecular weight above 20 kDa the melting temperature seems to remain constant. This is an indication for similar crystal thicknesses, i.e. possible chain folding. Analysis of the long period with increasing molecular weight (Fig.4b) confirms this fact. Up to 20 kDa the long period increases, i.e. the peak is shifted to lower q. Then the dependence is clearly reversed. Furthermore the peak is much less strong.

More detailed analysis is under way in order to fully understand phase transitions and chain folding taking place in P3HT. Moreover a detailed analysis of the wide angle scattering data is aimed at determining the crystallinity. Hereby we want to understand the molecular weight dependence of the crystallinity. These results will be useful to establish the relation between structure and morphology of P3HT on one hand and electronic properties on the other hand.

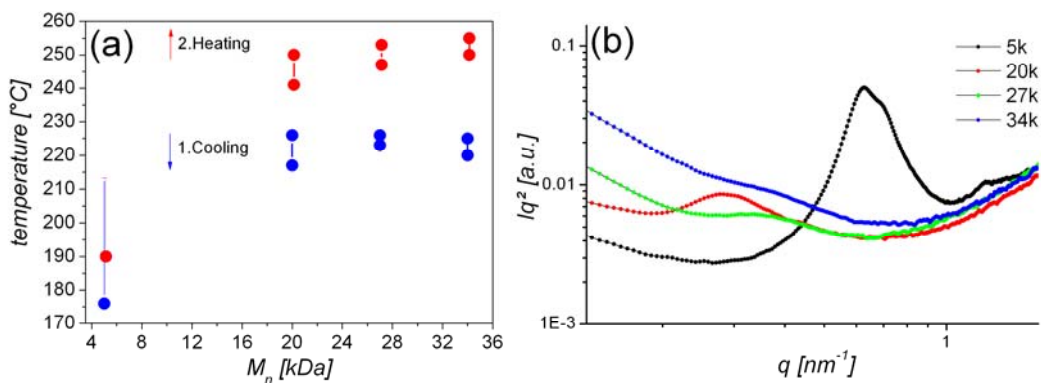


Fig 11- a) Temperature ranges at which the liquid crystalline phase for regioregular poly(3-hexyl thiophene)s were observed. (b) Parts of small angle scattering curves for different molecular weights of P3HT powders indicating the semicrystalline structure, i.e. the position of the peak maximum corresponds to the long period d_l of the lamellae.

For example, we want to correlate this melting (Figure 12a) and crystallisation (Figure 12b) process with the optical changes obtained from temperature dependent UV-Vis absorption spectroscopy. (Figure 12c). The vibronic progressions visible in Figure 12c are a result of the P3HT crystallisation. The planarization of the conjugated thiophene units and the crystallisation into H-aggregates leads to a pronounced red-shift, whereby the S0-0 transition at 610 nm is the most prominent feature indicating the enhanced crystallinity.

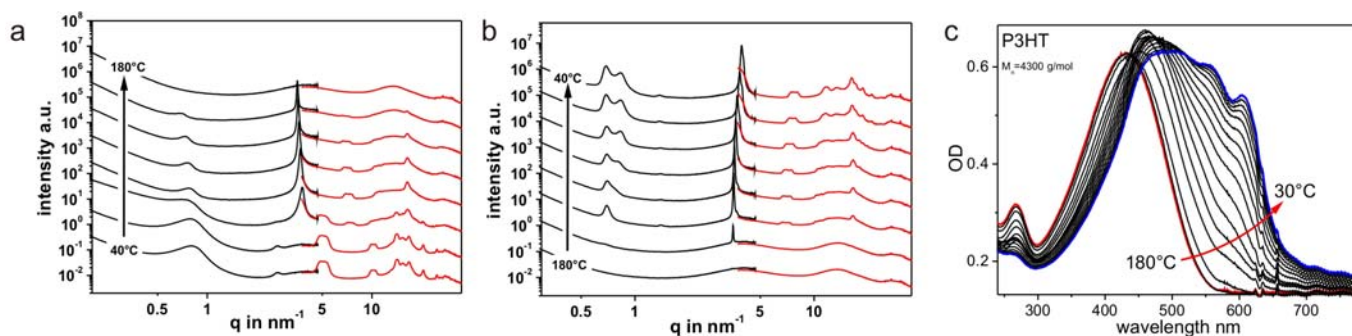


Fig 12- a) Heating and b) cooling of a P3HT sample $M_n=4.3$ kg/mol. c) Corresponding UV-Vis measurements showing optical changes during recrystallisation.

6) In-situ solvent vapour annealing (SVA) of P3HT

Another possibility to “melt” a polymer crystal is to expose the polymer to solvent vapour. Depending on the solubility, the interaction between solvent molecules and the monomer units of the polymer lead to the incorporation of solvent molecules into the polymer. This means that the polymer swells leading to dissolution of the crystalline areas of the polymer. The incorporation of solvent molecules introduces mobility to the polymer chains – comparable to a melt, although the mobility can be considerably higher. Therefore this method is especially interesting to anneal homopolymer and block copolymer thin films. A further advantage is that the process can be carried at mild conditions at room temperature, avoiding possible degradations of these organic electronic materials.¹¹

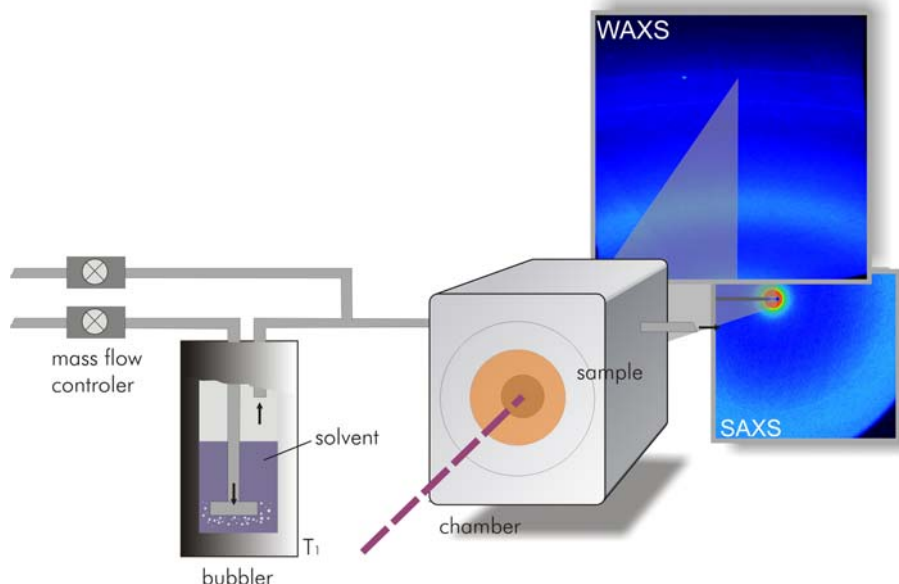


Fig 13 - Schematic of experimental setup. The solvent vapour atmosphere is controlled within a chamber with Kapton windows.

Figure 13 shows a schematic of the setup as it was used at ID02. The sample, which is small bulk sample of approx. 0.5-1 mm thickness, is mounted in a chamber with kapton windows. By controlling the flow of nitrogen gas through a wash bottle with solvent, we are able to adjust an accurate saturation of solvent vapour within the chamber. The following measurement demonstrates first results obtained from a P3HT with a molecular weight as low as 4.3 kg/mol. Fig. 14 shows the SAXS/WAXS spectra obtained at selected times at a saturation of 99% chloroform. Upon swelling, we can observe how the solvent interacts with the polymer chains. Most obviously, we found a difference depending on the molecular weight of P3HT. While the small molecular weight sample dissolved relatively fast, it took longer for a higher molecular weight one (e.g. $M_n = 22\text{kg/mol}$). Furthermore it was observable that the amorphous parts of the semicrystalline sample take up the solvent first and then slowly “melt” the polymer crystals. There is a difference in the “melting” behaviour depending on the molecular weight. Upon solvent exposure, the $M_n = 22\text{ kg/mol}$ P3HT shows an increasingly pronounced peak ($q = 0.26\text{ nm}^{-1}$) in the long period L, showing that amorphous parts absorb solvent molecules and allow for a better rearrangement of amorphous and crystalline parts. Also, the side chains start to swell and distances between chains increase, leading to an increase of the lamellar spacing (100 peak at $q = 3.1\text{ nm}^{-1}$ shifts to smaller q values). After prolonged solvent vapour uptake complete dissolution of the crystals can be observed in the vanishing of the π - π -stacking peak ($q = 16.5\text{ nm}^{-1}$), the lamellar (100) peak and the long period L.

The sample with the lower molecular weight shows a different behaviour. Firstly, the long period is reflected very pronounced (here two peaks are seen, which is under investigation). Upon solvent vapour uptake, it seems that the previously crystalline alkyl chains adapt another phase leading to the appearance of a new peak left of the (100) peak. Additionally, a further peak in the long period appears. However, during this

¹¹ Hüttner, S.; Sommer, M.; Chiche, A.; Krausch, G.; Steiner, U. & Thelakkat, M. - *Soft Matter*, **2009**, 5, 4206-4211

transition process two distinct structures seem to be prevalent at the same time. There is no shift or slow transition of the new peaks, but we observe the appearance of complete new scattering features. After approximately 45 min of solvent vapour exposure the solvent uptake is that high, that we only observe an amorphous sample.

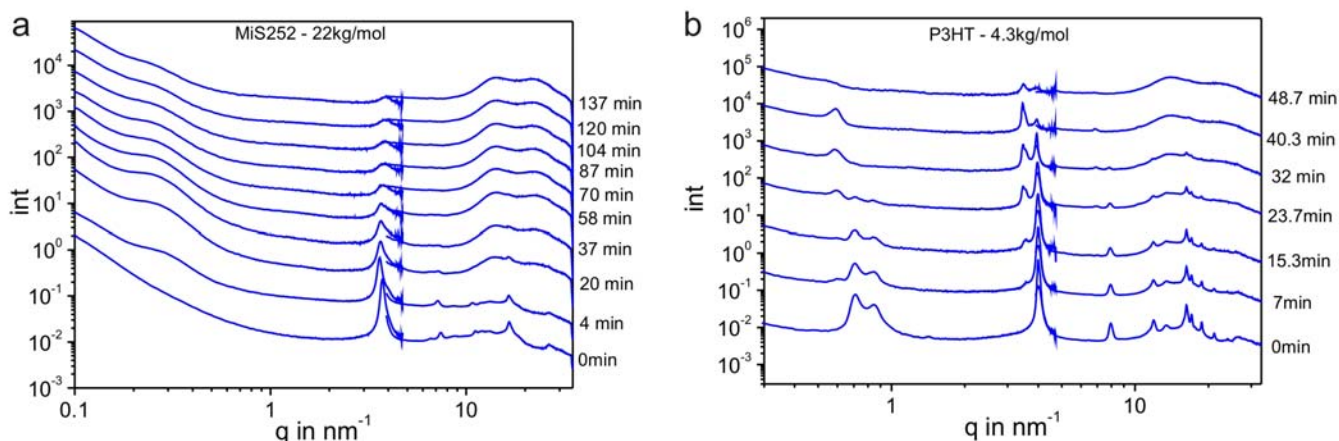


Fig 14 - Swelling of a P3HT sample with chloroform vapour. The time of swelling is indicated on the right. a) P3HT with $M_n = 22$ kg/mol, b) $M_n = 4.3$ kg/mol.

Defect-free poly(3-hexylthiophene)

In a very first measurement we tested the crystallinity of a novel synthesized poly(3-hexylthiophene) that shows 100% regioregularity (only head-to-tail couplings). This means, that all hexyl side chains are attached at the same position of the thiophene ring (Figure 15a). P3HT as synthesized with common methods only achieve maximum regio-regularities up to 98%. In some cases coupling defects are incorporated at the starting group of the polymer, but can also occur within the polymer (b). Such defects lead to a twist in the planarity of the polymer backbone to avoid sterical hindrance, and limit the overall degree of crystallinity. Finally, we note that such defects can have severe impacts on the device performance of photovoltaic cells¹².

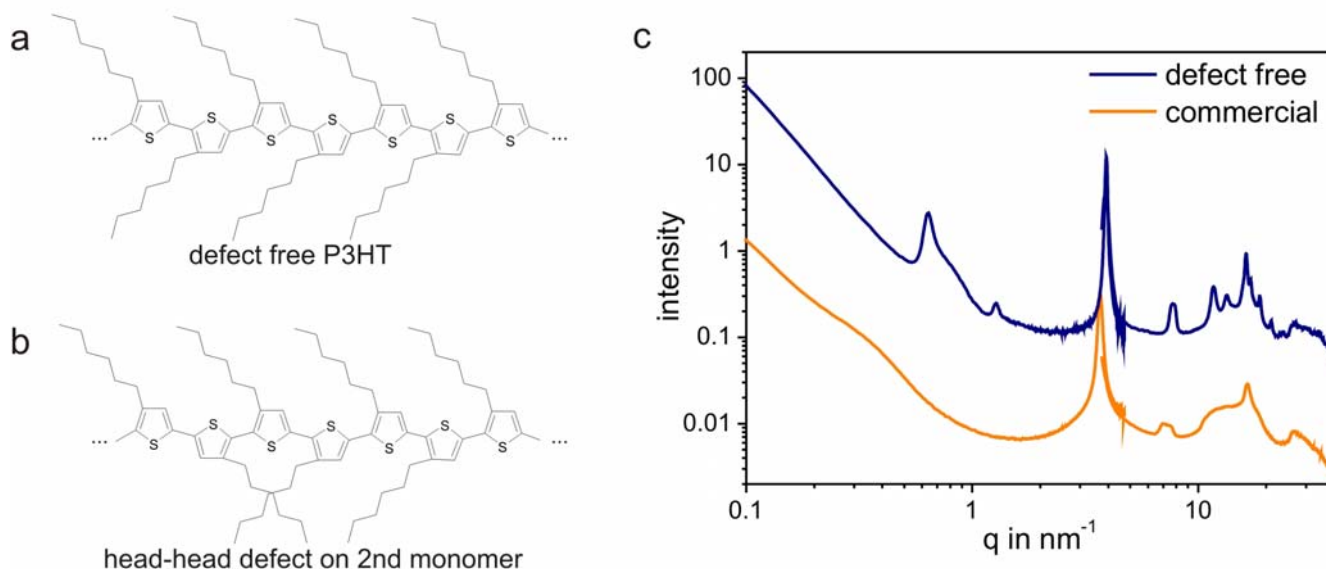


Fig 15 - Comparing a commercial P3HT with approx 96% and large polydispersity to a defect free P3HT with low polydispersity. The commercial sample shows a broad feature in the SAXS region. The shape of this peak is dependent on the molecular weight, but also on polydispersity and the number of defects within the chain. The defect-free P3HT with low molecular weight and small polydispersity shows a higher order reflection of the long period, which is observed for P3HT for the first time here.

¹² Y. Kim, S. Cook, S.M. Tuladhar, S.A. Choulis, J. Nelson, J. Durrant, D.C. Bradley, M. Giles, I. McCulloch, C.-S. Ha, M. Ree – Nature Mater. 5, 197 (2006)

We therefore synthesized defect free P3HT with various molecular weights and very low polydispersity and carried out these first scattering measurements. Figure 15c show a preliminary SAXS/WAXS measurement of a defect free P3HT. The higher orders in the long period (L) are observed for the first time and indicate very sharp boundaries between the crystalline and amorphous parts. Together with very crystallinities observed in differential scanning calorimetry (DSC) measurements, these new materials exhibit unprecedented properties to be further investigated. An elaborate investigation of these polymers is therefore planned within the next proposal.

General conclusions and outlook

The ID02 beamline is perfectly suited for the needs of the materials investigated. The wide q-range is perfectly suited for the different hierarchical structures we need to resolve. Scattering at the ESRF became an important method within our research of new materials. We therefore plan to apply for further beamtime in the future. As we are interested in organic electronic devices such as solar cells or transistors we also plan to extend our investigations to thin films i.e. using grazing incidence X-ray scattering.

Our ultimate goal is to obtain structure – function relations of new materials for organic electronics such as functionalized block copolymers that bear both, hole conducting as well as electron conducting blocks. Thereby, the hole conducting blocks can be either amorphous or crystalline. We have now achieved preliminary temperature-dependent scattering data as well as the influence of solvent vapour exposure. We are very satisfied with the results obtained within the first and second proposal and look forward to continue this project. We have already implicated important results acquired at the ID2 in advanced synthetic methods, which finally enables us to make better materials. This positive feedback is very important for our future research and motivates us to continue in this direction. The first publications are now online, several publications are in preparation or have already been submitted.

Abstracts of papers in progress:

Synthesis and Characterization of Monocarboxylated Poly(3-hexylthiophene)s via Quantitative End-Group Functionalization – R. Lohwasser et al. *Macromolecules*, 2010, DOI: 10.1021/ma1013258

We report the quantitative conversion of bromine end groups in regioregular poly(3-hexylthiophene)s (P3HTs) and the characterization of the resulting monocarboxylated P3HTs (P3HT-COOHs) carrying one carboxylic acid group at their chain ends. The monocarboxylation for three different chain lengths is carried out, and the resulting P3HT-COOHs are characterized with size exclusion chromatography, matrix-assisted laser desorption ionization spectroscopy with time-of-flight detection mass spectroscopy, and UV-vis spectroscopy. The thermal properties and crystallinity in bulk and thin films were studied in a comparison between P3HT and P3HT-COOHs. Differential scanning calorimetry and wide-angle X-ray scattering support the increasing crystallinity for the higher molecular weight samples. Preliminary OFET measurements show a good charge carrier mobility in the range of 10^{-3} cm²/(V s) for P3HT-COOHs with molecular weights of 5000 and 10800 g/mol.

Crystallization induced phase separation in poly(3-hexyl thiophene)-block-poly(perylene bisimide acrylate) donor-acceptor block copolymer – P. Kohn et al., *Macromolecules*, submitted.

We report about temperature dependent X-ray scattering experiments on a donor-acceptor block copolymer comprising poly(3-hexyl thiophene) and poly(perylene bisimide acrylate) subchains in bulk. At high temperatures the donor and acceptor segments are not separated into microphases and only the crystallization

of both components introduces a lamellar morphology. Analysis of the width of the Bragg-reflections of the poly(perylene bisimide acrylate) lattice indicates an orientation of the π - π -stacking direction approximately parallel to the lamella normal. Based on packing considerations we give a possible explanation for such an orientation. The results suggest that for optimal bipolar charge transport properties both - the relative crystal orientation as well as the microphase orientation - need to be controlled.

Intermolecular Interactions in Perylene Bisimide Polymer Architectures with Increasing Complexity – S. Huettner et al., in preparation.

This work focuses on a set of perylene bisimide (PBI) based homo- and block copolymers, able to serve as model materials in the study of self-organising properties of PBI moieties. The possibility of utilising the films of these block copolymers as photoactive components in organic photovoltaic devices is addressed by detailed spectroscopic and structural characterisation studies. The tendency of these compounds to self-organise in the solid state is addressed in a step-wise fashion by increasing the complexity of the chemical structure, from a monomer (Per), to a polymer (poly(perylene bisimide acrylate) - PPerAcr), to a block copolymer with an inert polystyrene block (PS-*b*-PPerAcr), and finally to a block copolymer carrying a donor block of poly(vinyltriphenylamine) PvTPA-*b*-PPerAcr. The PBI moieties exhibit strong π - π interactions, affecting the optical and electronic properties, but also its semi-crystalline structure. The factors that dictate the extent of mesoscopic order in PPerAcr films are discussed based on in situ temperature-dependent small and wide angle x-ray scattering, combined with absorption spectroscopy. Evidence for long range order is presented for these superstructures when appropriate thermal processing protocols are adapted, which improves the electron charge carrier mobility. The formation of longer aggregates is related to a decrease in the photoluminescence and a prolonged exciton polarization anisotropy measured by time resolved transient absorption spectroscopy. Further, modified patterns of hierarchical organisation in the solid state are found when block-units of electronically inactive polystyrene (PS) are linked to PPerAcr (PS-*b*-PPerAcr). Block copolymer morphologies such as lamellae and cylinders could be identified by small angle X-ray scattering depending on the block copolymer composition. The mesoscopic order and the optical properties of the PBI moieties stay unaffected by the confinement in these microphases. The effect of annealing regarding the interplay between morphological order and intermolecular packing of the PBIs was studied.

Finally, photovoltaic active PPerAcr-*b*-PvTPA block copolymers are obtained when the PS block is replaced by the hole conducting poly(vinyltriphenylamine). The photovoltaic performance of PvTPA-*b*-PPerAcr, however, strongly depends on both, the crystallinity and the morphology of a donor-acceptor system. The crystallinity can be increased locally by thermal annealing already below its melting temperature, increasing the electron mobility as well as the external quantum efficiency.

Tuneable Charge Transport Using Supramolecular Self-Assembly of Nanostructured Crystalline Block Copolymers – S. Huettner et al., submitted to ACS Nano

Electronically functionalized block copolymers, combining covalently linked p-type and n-type blocks, show switching behaviour of charge transport in organic field effect transistors (OFETs). The electronically active subunits self-assemble into continuous microdomains, thereby forming percolation channels for holes or electrons or both depending on the composition and processing conditions. Here, we establish a charge transport - morphology relation for donor-acceptor block copolymers with two crystalline blocks. The n-type and p-type blocks self-assemble into two-dimensional lattices of π - π stacks and main chain polymer lamella, respectively, over a broad composition range. Controlling the crystallization preferences of the two blocks by thermal annealing allows controlling the OFET polarity. Depending on the block ratio, the charge transport can be tuned from p-type to n-type or p-type to ambipolar, respectively.